

The following resources related to this article are available online at www.sciencemag.org (this information is current as of November 9, 2009):

Updated information and services, including high-resolution figures, can be found in the online version of this article at:

<http://www.sciencemag.org/cgi/content/full/310/5756/1954>

Supporting Online Material can be found at:

<http://www.sciencemag.org/cgi/content/full/310/5756/1954/DC1>

A list of selected additional articles on the Science Web sites **related to this article** can be found at:

<http://www.sciencemag.org/cgi/content/full/310/5756/1954#related-content>

This article **cites 30 articles**, 10 of which can be accessed for free:

<http://www.sciencemag.org/cgi/content/full/310/5756/1954#otherarticles>

This article has been **cited by** 72 article(s) on the ISI Web of Science.

This article has been **cited by** 19 articles hosted by HighWire Press; see:

<http://www.sciencemag.org/cgi/content/full/310/5756/1954#otherarticles>

This article appears in the following **subject collections**:

Physiology

<http://www.sciencemag.org/cgi/collection/physiology>

Information about obtaining **reprints** of this article or about obtaining **permission to reproduce this article** in whole or in part can be found at:

<http://www.sciencemag.org/about/permissions.dtl>

A Developmental Timing MicroRNA and Its Target Regulate Life Span in *C. elegans*

Michelle Boehm and Frank Slack*

The microRNA *lin-4* and its target, the putative transcription factor *lin-14*, control the timing of larval development in *Caenorhabditis elegans*. Here, we report that *lin-4* and *lin-14* also regulate life span in the adult. Reducing the activity of *lin-4* shortened life span and accelerated tissue aging, whereas overexpressing *lin-4* or reducing the activity of *lin-14* extended life span. Life-span extension conferred by a reduction in *lin-14* was dependent on the DAF-16 and HSF-1 transcription factors, suggesting that the *lin-4*–*lin-14* pair affects life span through the insulin/insulin-like growth factor–1 pathway. This work reveals a role for microRNAs and developmental timing genes in life-span regulation.

Life span is highly variable among species, and it has become clear that a genetic program of senescence in the soma is responsible for this variation (1). Recent studies have suggested that gene expression changes in the aged adult are developmentally timed at the transcriptional level. For example, in both the nematode *Caenorhabditis elegans* and the fly *Drosophila melanogaster*, a characteristic gene expression profile associated with age can be detected in young adulthood, well before the accumulation of molecular damage has begun (2). Thus, conserved genes may act temporally to initiate a program of aging that starts early in adult life (3, 4). We hypothesized that if such an aging program exists, it may be controlled by mechanisms similar to those used in developmental timing (3). The heterochronic genes of *C. elegans* constitute one such genetic pathway that regulates developmental timing (5–7).

Heterochronic genes, such as *lin-4* and *lin-14* (5, 8, 9), are temporal identity genes that affect the fate choices that cells make at specific times during development, and mutations in heterochronic genes result in temporal alterations to stage-specific patterns of cellular development (6, 7). Expression of the *lin-4* microRNA (miRNA) is up-regulated near the end of the first larval stage, and *lin-4* binds with imperfect complementarity to the 3'UTR of its target, *lin-14*, to prevent its translation (8–11) and allow stage two larval cell fates to occur. The molecular function of *lin-14* is unknown, but it encodes a nuclear protein (12) that associates with DNA (13) and has sequence similarities to transcription factors (fig. S1). LIN-14 is down-regulated

in the hypodermis at the first to second larval-stage transition (12), but its expression persists weakly in other tissues throughout larval development (13) and into adulthood (fig. S2). Similarly, *lin-4* is also expressed in the adult (14, 15) (fig. S2). Although the roles of *lin-4*

and *lin-14* during larval development have been extensively studied, the function of these genes in the adult has not been investigated. Therefore, we tested whether genes that direct the timing of early developmental events may also function in the adult to regulate the timing of later processes, such as life span and aging.

We assayed heterochronic mutants for life-span length and found that mutations in *lin-4* and *lin-14* resulted in aging defects. Animals with a loss-of-function (*lf*) mutation in *lin-4* displayed a life span that was significantly shorter than that of the wild type (Fig. 1A), suggesting that *lin-4* is required to prevent premature death. Conversely, overexpressing *lin-4* from an extrachromosomal array led to a lengthened life span (Fig. 1C). This result demonstrates that the *lin-4* (*lf*) mutant did not die prematurely solely as the result of an unrelated, general pathology, but rather that *lin-4* functions to extend life span. Consistent with our *lin-4* data, we found that a *lf* mutation in a target of *lin-4*, *lin-14*, produced the opposite life-span phenotype. Animals carrying a temperature-sensitive *lf* mutation in *lin-14* had a 31% longer life span than the wild type (Fig. 1B). The longevity

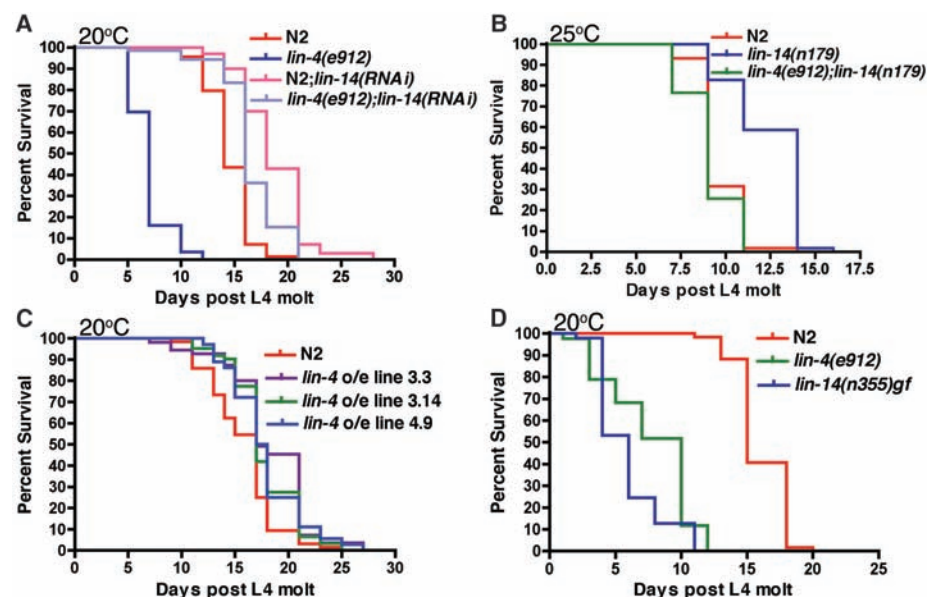


Fig. 1. *lin-4* and *lin-14* mutants have opposite life-span phenotypes. (A) Red, survival of wild-type (N2) animals on control bacteria containing empty vector (mock RNAi); blue, *lin-4*(*e912*)*lf*; mock RNAi; pink, *lin-14*(RNAi); light blue, *lin-4*(*e912*)*lf*; *lin-14*(RNAi) at 20°C. N2: $n = 69$, $m = 14.6$. *lin-4*(*e912*)*lf*: $n = 56$, $m = 6.9$, $P < 0.0001^*$. N2;*lin-14*(RNAi): $n = 68$, $m = 18.7$, $P < 0.0001^*$. *lin-4*(*e912*)*lf*; *lin-14*(RNAi): $n = 72$, $m = 16.6$, $P < 0.0001^*$. (B) A *lin-14*(*lf*) mutation extends life span when grown and assayed at the restrictive temperature of 25°C. N2: $n = 57$, $m = 9.5$. *lin-14*(*n179*)*lf*: $n = 58$, $m = 12.5$, $P < 0.0001^*$. *lin-4*(*e912*)*lf*; *lin-14*(*n179*)*lf*: $n = 51$, $m = 9.0$, $P = 0.0906^*$. (C) *lin-4* overexpression extends life span. Three lines overexpressing (o/e) *lin-4* are shown in purple, blue, and green; wild-type animals are in red. N2: $n = 64$, $m = 15.8$. *lin-4* o/e line 3.3: $n = 54$, $m = 18.3$, $P < 0.0001^*$. *lin-4* o/e line 3.14: $n = 62$, $m = 17.7$, $P = 0.0023^*$. *lin-4* o/e line 4.9: $n = 37$, $m = 17.8$, $P = 0.0113^*$. (D) A *lin-14* gain-of-function mutant, *n355*, has a short-lived phenotype similar to that of the *lin-4*(*e912*)*lf* mutant. Red, wild-type animals; green, *lin-4*(*e912*)*lf*; blue, *lin-14*(*n355* *gf*). N2: $n = 59$, $m = 15.9$. *lin-4*(*e912*)*lf*: $n = 85$, $m = 7.7$, $P < 0.0001^*$. *lin-14*(*n355* *gf*): $n = 94$, $m = 5.9$, $P < 0.0001^*$. All experiments were repeated at least once with similar effects. n , number of animals observed in each experiment. m , mean adult life span (days). P^* values refer to experimental strain and N2 control animals in a single experiment, and $P\#$ values refer to a strain on control and experimental RNAi treatment in a single experiment.

Department of Molecular, Cellular, and Developmental Biology, Yale University, New Haven, CT 06511, USA.

*To whom correspondence should be addressed. E-mail: frank.slack@yale.edu

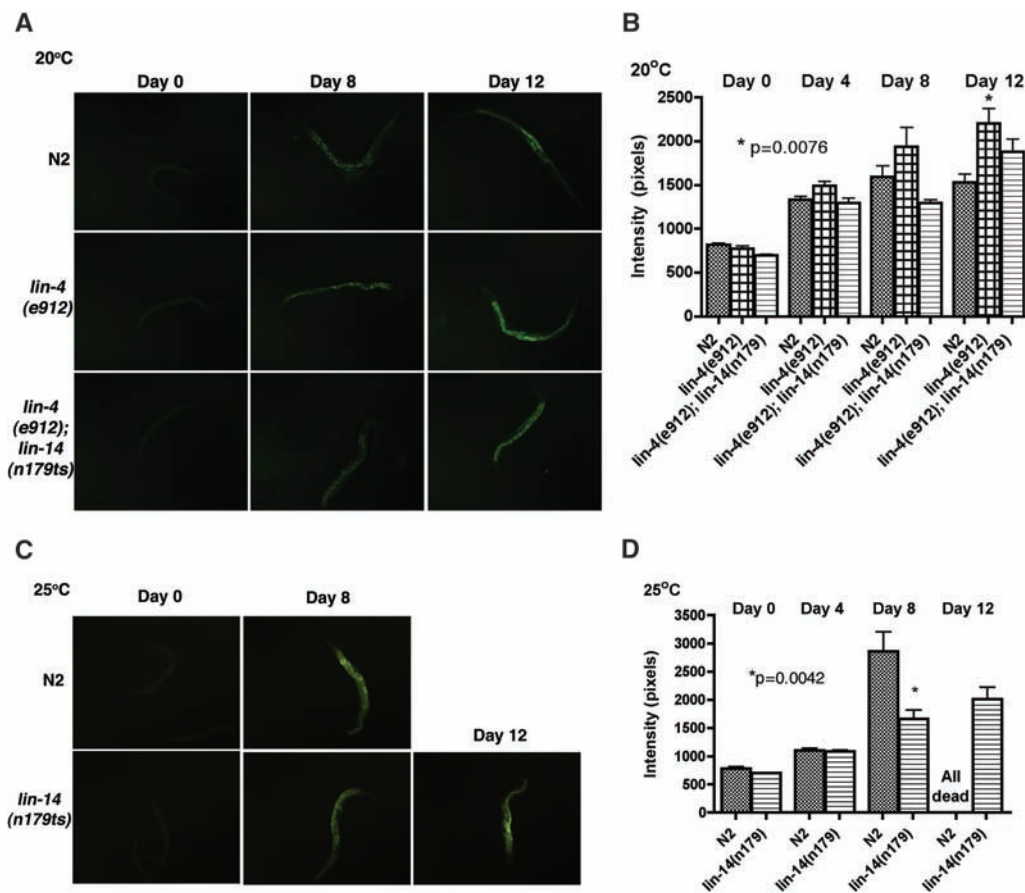


Fig. 2. *lin-4* and *lin-14* mutants display accelerated and delayed rates, respectively, of lipofuscin accumulation. (A) *lin-4(e912)lf* mutants display an increase of lipofuscin as compared with similarly aged wild-type animals at 20°C. This effect is suppressed by the *lin-14(n179)lf* mutation. (B) Quantification of the N2, *lin-4(e912)lf*, *lin-4(e912)lf;lin-14(n179)lf* populations' gut autofluorescence at days 0, 4, 8, and 12 after the larval-to-adult transition at 20°C. (C) *lin-14(n179)lf* mutants display a decrease in lipofuscin accumulation compared with wild-type animals at 25°C. (D) Quantification of the N2 and *lin-14(n179)lf* populations' gut autofluorescence at 25°C as for (B). For (A) and (C), photographs shown are representative examples ($n = 10$ for each time point per strain). Photographs were taken at 100 \times magnification. All animals were photographed on the same day under identical conditions, and photographs were treated identically. For (B) and (D), autofluorescence was quantified using Axiovision 4.4 software ($n = 10$ for each time point per strain). P values were calculated using the Mann-Whitney nonparametric t test comparing mutant to wild-type results at day 12 in (B) and day 8 in (D). Error bars represent the standard error of the mean.

phenotype produced by the *lin-14(lf)* lesion was reproduced by RNA interference (RNAi) of *lin-14* (Fig. 1A). Thus, *lin-14* normally acts to promote a short life span. A *lin-14* gain-of-function (*gf*) mutant (16), which lacks the *lin-14* complementary sites in the *lin-14* 3' untranslated region (UTR) and overexpresses LIN-14 at later stages (12), closely phenocopied the short-lived phenotype of the *lin-4(lf)* mutant (Fig. 1D). Additionally, *lin-14(RNAi)* suppressed the short life span of the *lin-4(e912)lf* mutant (Fig. 1A). Taken together, the data suggest that the major role of *lin-4* in regulating life span is to repress its target, *lin-14*.

To determine whether the short life span of *lin-4(lf)* mutants is due to accelerated aging or to an unrelated, pleiotropic cause, we monitored the accumulation of intestinal autofluorescence in adult animals. Intestinal autofluorescence, which is caused by lysosomal deposits of lipofuscin, accumulates over time in the aging animal and is an established marker for aging (17). In agreement with its short life span, the *lin-4(lf)* mutant accumulated intestinal autofluorescence more rapidly than the wild type (Fig. 2, A and B). These results resemble those found for the short-lived strain with a *daf-16(lf)* mutation (fig. S3, A and B). *daf-16* encodes a FOXO transcription factor that regulates life span through insulin-like signaling (1, 18–20). The premature lipofuscin accumulation caused

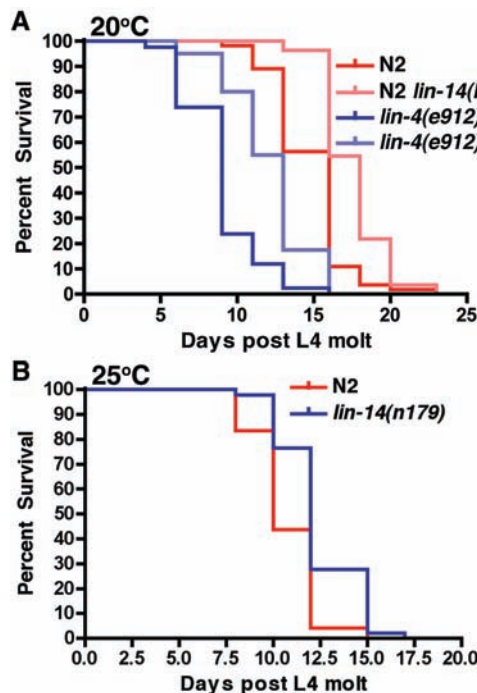


Fig. 3. Loss of *lin-14* function during adulthood is sufficient to extend life span. (A) Wild-type animals treated with *lin-14(RNAi)* (pink) only in the adult stage have extended life spans compared with mock RNAi animals (red). *lin-4(e912)lf* mutants treated with *lin-14(RNAi)* (light blue) only in the adult stage display an extended life span compared with *lin-4(e912)lf* mutants on mock RNAi (blue) at 20°C. N2: $n = 55$, $m = 14.8$. *lin-14(RNAi)*: $n = 55$, $m = 17.6$, $P < 0.0001^*$. *lin-4(e912)lf*: $n = 43$, $m = 9.0$. *lin-4(e912)lf; lin-14(RNAi)*: $n = 40$, $m = 12.1$, $P < 0.0001^{\#}$. (B) *lin-14(n179)lf* animals (blue) display extended life spans compared with wild-type animals (red) when grown at the permissive temperature of 15°C until the larval-to-adult transition and then moved to the restrictive temperature of 25°C. N2: $n = 48$, $m = 10.7$. *lin-14(n179)lf*: $n = 53$, $m = 12.4$, $P < 0.0001^*$. All experiments were repeated at least once with similar effects. P^* and $P^{\#}$ are defined in the legend to Fig. 1.

by *lin-4(lf)* was suppressed when combined with the *lin-14(n179)lf* lesion (Fig. 2, A and B), consistent with the ability of *lin-14(lf)* to suppress the short life span of the *lin-4(lf)* mutant.

In contrast to *lin-4(lf)*, the *lin-14(n179)lf* mutant displayed a slower rate of intestinal autofluorescence accumulation as compared with the wild type (Fig. 2, C and D), in agreement with

its extended life span. The decreased rate of gut autofluorescence accumulation is similar to that observed in the long-lived *daf-2(lf)* mutant (fig. S3, C and D) (17). *daf-2* encodes an insulin/insulin-like growth factor-1 (IGF-1) receptor that lies upstream of *daf-16* in insulin-like signaling (18, 20, 21).

The stress response of the *lin-4(lf)* and *lin-14(lf)* strains was also examined. *C. elegans* mutants that display life-span phenotypes also display altered responses to stress treatments, including heat shock (22, 23). For instance, the long-lived *daf-2(lf)* mutant is highly tolerant to heat shock, and this heightened stress resistance is believed to be essential for life-span extension (22). In accordance with its life-span phenotype, the *lin-4(e912)lf* mutant displayed a greater sensitivity to heat shock as compared with the wild type (fig. S4B), whereas the *lin-14(n179)lf* mutant displayed a greater resistance to heat shock as compared with the wild type (fig. S4C).

To rule out the possibility that life-span modulation directed by *lin-14* and *lin-4* is merely due to their role in larval development, we examined the effect of reducing the function of *lin-14* only in the postmitotic adult. RNAi-mediated inhibition of *lin-14* expression after the final larval molt extended the life span of wild-type animals, similar to the extension observed when animals were exposed to *lin-14(RNAi)* just after hatching (Fig. 3A). Additionally, growing the *lin-14(n179)lf* mutant at the permissive temperature until young adulthood and then shifting to the restrictive temperature also produced an extended life span (Fig. 3B). These results demonstrate that *lin-14* functions in the adult to restrict life span. Furthermore, the short life span of the *lin-4(e912)lf* mutant was also rescued to a significant extent when exposed to *lin-14(RNAi)* only during adulthood. This result supports the idea that the *lin-4(e912)lf* accelerated-aging phenotype is not due to developmental abnormalities or an unrelated pleiotropic cause. Thus, the *lin-4* miRNA appears to suppress senescence in *C. elegans* through repression of *lin-14* in the adult.

We tested whether *lin-4* and *lin-14* extend life span by acting through one of the known *C. elegans* life-span regulatory pathways, such as the insulin/IGF-1 signaling pathway. Several insulin/IGF-1 signaling pathway members regulate life span through mechanisms dependent on the downstream DAF-16/FOXO and HSF-1 transcription factors (1, 18–21, 24, 25). As with *lin-4*, inhibiting *daf-16* or *hsf-1* activity shortens life span, whereas elevating their activity lengthens life span (25, 26). The *daf-16(mu86)* null mutant strain, when treated with *lin-14(RNAi)*, did not display an extended life span (Fig. 4B), nor did *lin-14(n179)lf; daf-16(RNAi)* animals (Fig. 4A). These data demonstrate that *daf-16* is required for the *lin-14(lf)*-mediated longevity phenotype. *lin-4(lf)* animals

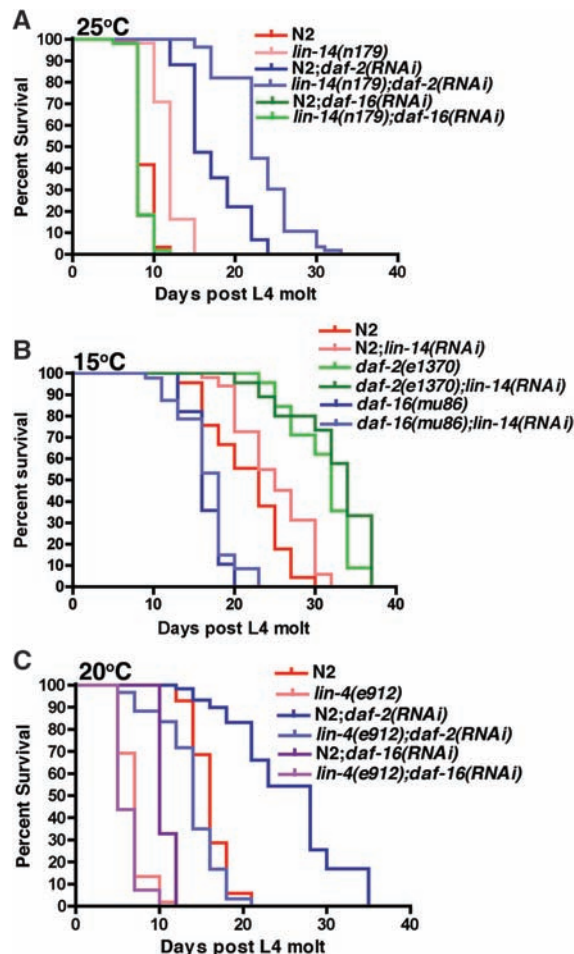


Fig. 4. The life-span extension of a *lin-14(lf)* mutant is *daf-16* dependent. (A) The life-span extension conferred by the *lin-14(n179)lf* mutation is abolished with *daf-16(RNAi)* (light green); *daf-16(RNAi)* animals (green—obscured by light green). *lin-14(lf); daf-2(RNAi)* (light blue) displays a further lengthening of the life-span extension conferred by *daf-2(RNAi)* (blue) at 25°C. Wild-type (red) and *lin-14(n179)lf* (pink) animals on mock RNAi are shown for comparison. N2: $n = 60$, $m = 8.9$. *lin-14(n179)lf*: $n = 56$, $m = 11.9$, $P < 0.0001^*$. *daf-2(RNAi)*: $n = 58$, $m = 17.1$. *lin-14(n179)lf; daf-2(RNAi)*: $n = 56$, $m = 23.0$, $P < 0.0001^*$. *daf-16(RNAi)*: $n = 55$, $m = 8.3$. *lin-14(n179)lf; daf-16(RNAi)*: $n = 54$, $m = 8.4$, $P = 0.9330^*$. (B) *lin-14(RNAi)* is unable to extend the life span of *daf-16(mu86)* (light blue) or *daf-2(e1370)lf* (light green) mutants as compared with these strains grown on mock RNAi (blue and green, respectively) at 15°C. Wild-type animals on mock RNAi (red) and on *lin-14(RNAi)* (pink) are shown for comparison. N2: $n = 45$, $m = 21.6$. *lin-14(RNAi)*: $n = 51$, $m = 25.1$, $P = 0.0003^*$. *daf-2(e1370)lf*: $n = 49$, $m = 32.3$. *daf-2(e1370)lf; lin-14(RNAi)*: $n = 53$, $m = 31.1$, $P = 0.0100\#$. *daf-16(mu86)*: $n = 28$, $m = 16.4$. *daf-16(mu86); lin-14(RNAi)*: $n = 42$, $m = 16.7$, $P = 0.2300\#$. (C) A wild-type copy of *lin-4* is required for full life-span extension by *daf-2(RNAi)* (blue versus light blue), and is also required for the life-span phenotype conferred by *daf-16(RNAi)* (purple versus light purple). Wild-type (red) and *lin-4(e912)lf* (pink) animals grown on mock RNAi are shown for comparison. N2: $n = 70$, $m = 16.0$. *lin-4(e912)lf*: $n = 52$, $m = 6.8$, $P < 0.0001^*$. *daf-2(e1370)*: $n = 67$, $m = 25.5$. *lin-4(e912)lf; daf-2(RNAi)*: $n = 55$, $m = 13.8$, $P < 0.0001^*$. *daf-16(RNAi)*: $n = 64$, $m = 10.7$. *lin-4(e912)lf; daf-16(RNAi)*: $n = 55$, $m = 6.1$, $P < 0.0001^*$. All experiments were repeated at least once with similar results. P^* and $P\#$ are defined in the legend to Fig. 1.

grown on *daf-16(RNAi)* had shortened life-span lengths that are identical to that of the *lin-4(lf)* strain grown on mock RNAi (Fig. 4C), indicating that *lin-4* and *lin-14* genetically interact with *daf-16*. However, the *lin-4(lf)* mutant had a shorter life span than the *daf-16(lf)* mutant, indicating that *lin-14* does not exert its effect on life span by negative regulation of DAF-16 alone. Consistent with this idea, the *lin-14(lf); hsf-1(RNAi)* animals had a short life span, indicating that the *lin-14(lf)*-mediated longevity phenotype is dependent on *hsf-1* (fig. S4A) as well as on *daf-16*.

To further explore the possibility that *lin-4* and *lin-14* might function through the insulin/IGF-1 pathway, we analyzed their interactions with the *daf-2*-insulin/IGF-1 receptor. Consistent with previous studies, *daf-2(RNAi)* animals had a significant extension in life span compared with wild-type animals (Fig. 4C) (25). This life-span extension was significantly reduced by the *lin-4(e912)lf* lesion (Fig. 4C), such that *lin-4(e912)lf; daf-2(RNAi)* animals displayed life spans similar to those of

the wild type. This phenotype is different from that of the *hsf-1(lf)* mutation, which wholly abolishes the life-span extension conferred by *daf-2(lf)* and results in a shortened life span (25). An epistatic relationship between *lin-4* and *daf-2* cannot be determined because the *daf-2* allele is non-null. However, our data suggests that a wild-type copy of *daf-2* is necessary for the short life span phenotype conferred by *lin-4(lf)*. The life span of the *daf-2(e1370)lf* mutant was modestly extended by *lin-14(RNAi)* (Fig. 4B), and *lin-14(n179)lf; daf-2(RNAi)* animals also displayed an extended life span as compared with *daf-2(RNAi)* animals (Fig. 4A). Null alleles were not used for either analysis, and thus concrete epistatic relationships cannot be determined. However, our data support a model whereby *lin-4* and *lin-14* modulate life span through the canonical *daf-2* insulin/IGF-1 pathway. Alternatively, *lin-4* and *lin-14* may converge onto the DAF-16/FOXO transcription factor in a pathway parallel to the *daf-2* insulin/IGF-1 pathway to control aging.

In key *C. elegans* adult tissues, the *lin-4* miRNA may act to suppress the translation of *lin-14*, preventing *lin-14* from affecting the transcription of a yet unidentified factor that regulates or interacts with the *daf-2* insulin/IGF-1 pathway. By demonstrating that *lin-4* and *lin-14*, two key temporal regulators of development, also influence the rate of aging, we provide support for the theory that life span is affected by an innate, programmed timing mechanism. However, our data are also consistent with an alternative theory of aging, antagonistic pleiotropy, which posits that genes with primary roles in development can later secondarily influence life span (27). miRNAs are important regulators of development, apoptosis, and metabolism (28–31), and our work demonstrates that a miRNA can regulate aging, possibly through the insulin-like signaling pathway. It is possible that the mammalian *lin-4* miRNA homologs, the *miR-125* family, may regulate processes responsible for life-span determination in vertebrates.

fgf20 Is Essential for Initiating Zebrafish Fin Regeneration

Geoffrey G. Whitehead, Shinji Makino, Ching-Ling Lien, Mark T. Keating*

Epimorphic regeneration requires the presence or creation of pluripotent cells capable of reproducing lost organs. Zebrafish fin regeneration is mediated by the creation of blastema cells. Here, we characterize the *devoid of blastema* (*dob*) mutant that fails fin regeneration during initial steps, forms abnormal regeneration epithelium, and does not form blastema. This mutation has no impact on embryonic survival. *Dob* results from an *fgf20a* null mutation, Y148S. *Fgf20a* is expressed during initiation of fin regeneration at the epithelial-mesenchymal boundary and later overlaps with the blastema marker *msxb*. Thus, *fgf20a* has a regeneration-specific requirement, initiating fin regeneration, and controlling blastema formation.

Vertebrate regeneration is of scientific and medical interest. Although acute tissue regeneration in humans is limited, other vertebrates possess extraordinary regenerative capabilities. Zebrafish are amenable to genetic analyses and regenerate an impressive array of structures, including spinal cord, optic nerve, heart, and fins (1–3). Zebrafish fin regeneration is marked by five stages: regeneration epithelialization, mesenchymal disorganization, blastema formation, regenerative outgrowth, and termination. Although genetic analyses have enhanced our understanding of fin regeneration (1, 4–6), the

References and Notes

- C. Kenyon, *Cell* **120**, 449 (2005).
- S. A. McCarrroll et al., *Nat. Genet.* **36**, 197 (2004).
- C. Kenyon, in *C. elegans II: Monograph* 33, D. L. Riddle, Ed. (Cold Spring Harbor Laboratory, Plainview, New York, 1997), p. xvii, p. 796.
- T. Lu et al., *Nature* **429**, 883 (2004).
- V. Ambros, H. R. Horvitz, *Genes Dev.* **1**, 398 (1987).
- D. Banerjee, F. Slack, *Bioessays* **24**, 119 (2002).
- F. Slack, G. Ruvkun, *Annu. Rev. Genet.* **31**, 611 (1997).
- R. C. Lee, R. L. Feinbaum, V. Ambros, *Cell* **75**, 843 (1993).
- B. Wightman, I. Ha, G. Ruvkun, *Cell* **75**, 855 (1993).
- P. H. Olsen, V. Ambros, *Dev. Biol.* **216**, 671 (1999).
- R. Feinbaum, V. Ambros, *Dev. Biol.* **210**, 87 (1999).
- G. Ruvkun, J. Giusto, *Nature* **338**, 313 (1989).
- Y. Hong, R. C. Lee, V. Ambros, *Mol. Cell. Biol.* **20**, 2285 (2000).
- L. P. Lim et al., *Genes Dev.* **17**, 991 (2003).
- A. Esquela-Kerscher et al., *Dev. Dyn.* **234**, 868 (2005).
- B. Wightman, T. R. Burglin, J. Gatto, P. Arasu, G. Ruvkun, *Genes Dev.* **5**, 1813 (1991).
- D. Garigan et al., *Genetics* **161**, 1101 (2002).
- C. Kenyon, J. Chang, E. Gensch, A. Rudner, R. Tabtiang, *Nature* **366**, 461 (1993).
- K. Lin, J. B. Dorman, A. Rodan, C. Kenyon, *Science* **278**, 1319 (1997).
- P. L. Larsen, P. S. Albert, D. L. Riddle, *Genetics* **139**, 1567 (1995).
- K. D. Kimura, H. A. Tissenbaum, Y. Liu, G. Ruvkun, *Science* **277**, 942 (1997).
- G. J. Lithgow, T. M. White, S. Melov, T. E. Johnson, *Proc. Natl. Acad. Sci. U.S.A.* **92**, 7540 (1995).
- S. S. Lee et al., *Nat. Genet.* **33**, 40 (2003).
- S. Ogg et al., *Nature* **389**, 994 (1997).
- A. L. Hsu, C. T. Murphy, C. Kenyon, *Science* **300**, 1142 (2003).
- K. Lin, H. Hsin, N. Libina, C. Kenyon, *Nat. Genet.* **28**, 139 (2001).
- K. A. Hughes, R. M. Reynolds, *Annu. Rev. Entomol.* **50**, 421 (2005).
- D. P. Bartel, *Cell* **116**, 281 (2004).
- J. Brennecke, D. R. Hipfner, A. Stark, R. B. Russell, S. M. Cohen, *Cell* **113**, 25 (2003).
- M. N. Poy et al., *Nature* **432**, 226 (2004).
- B. J. Reinhart et al., *Nature* **403**, 901 (2000).
- We thank A. Esquela-Kerscher, D. Banerjee, and K. Carter for critical reading of this manuscript; K. Carter and L. Bai for providing the *zals1* strain; S. S. Lee for technical advice; and R. Lee and V. Ambros, and the *C. elegans* Genetic Center, for supplying strains. This work was supported by an NIH grant (GM64701) to F.S.

Supporting Online Material

www.sciencemag.org/cgi/content/full/310/5756/1954/DC1

Materials and Methods

Figs. S1 to S4

Table S1

References and Notes

1 June 2005; accepted 10 November 2005

10.1126/science.1115596

We expected that *dob* would also disrupt embryogenesis (1, 4–6). However, at 33°C, *dob* viability was comparable with wild type (fig. S1A). Half (23/46) of *dob* adults developed asymmetric caudal fin lobes when heat-shocked as embryos, yet all wild type (41/41) developed symmetric fin lobes (fig. S1B). The total size of wild-type and *dob* caudal fins was comparable (fig. S1B). Therefore, there appears to be an incompletely penetrant ts patterning defect in *dob* (8). Survival of *dob* adults at 33°C was also comparable to wild type (fig. S1C). These data suggest a regeneration-specific requirement for *dob*.

To determine the cellular nature of *dob* regenerative failure, we examined histology of regenerates at 33°C. The first stage of regeneration, formation of regeneration epithelium, appeared abnormal. At 6 and 12 hours post-amputation (*hpa*), *dob* regenerates demonstrated a thickened regeneration epithelium (Fig. 2A). Epithelial proliferation levels in *dob* at 6 and 12 *hpa* were similar to wild type (fig. S3A). Therefore, thickened regeneration epithelium likely results from aberrant epithelial migration (9, 10).

To determine whether *dob* resulted from a primary defect in wound healing, we performed a longitudinal incision along the caudal fin and allowed healing at 33°C. The wild-type response to this injury is nonregenerative, as the wound is covered by epithelium and leaves a slit down the fin. We found no difference in the timing, histochemistry, or bromodeoxyuridine (BrdU) immunohistochemistry of wound-healing between wild type and *dob* (fig. S3B). The possibility remains that the *dob* mutant may have a subtle defect in wound-healing not identified by our observations.

Howard Hughes Medical Institute, Department of Cell Biology, Harvard Medical School, Department of Cardiology, Children's Hospital, Boston, MA 02115, USA.

*To whom correspondence should be addressed. E-mail: mark.keating@novartis.com